Biochimica et Biophysica Acta 1837 (2014) 1122–1129

Contents lists available at ScienceDirect

Biochimica et Biophysica Acta

journal homepage: www.elsevier.com/locate/bbabio

Localization-controlled specificity of FAD:threonine flavin transferases in *Klebsiella pneumoniae* and its implications for the mechanism of Na^+-translocating NADH:quinone oxidoreductase ☆

Yulia V. Bertsova, Vitaly A. Kostyrko, Alexander A. Baykov, Alexander V. Bogachev *

Belozersky Institute of Physico-Chemical Biology, Lomonosov Moscow State University, Moscow 119992, Russia

ARTICLE INFO

Article history:
Received 30 October 2013
Received in revised form 4 December 2013
Accepted 13 December 2013
Available online 20 December 2013

Keywords:
Klebsiella pneumoniae
NADH:quinone oxidoreductase
Fumarate reductase
Flavin transferase
Na^+ transport
FMN

ABSTRACT

The *Klebsiella pneumoniae* genome contains genes for two putative flavin transferase enzymes (ApbE1 and ApbE2) that add FMN to protein Thr residues. ApbE1, but not ApbE2, has a periplasm-addressing signal sequence. The genome also contains genes for three target proteins with the Dxx(s/t)gAT flavinylation motif: two subunits of Na^+-translocating NADH:quinone oxidoreductase (Na^+-NQR), and a 99.5 kDa protein, KPK_2907, with a previously unknown function. We show here that KPK_2907 is an active cytoplasmically-localized fumarate reductase. *K. pneumoniae* cells with an inactivated *kpk_2907* gene lack cytoplasmic fumarate reductase activity, while retaining this activity in the membrane fraction. Complementation of the mutant strain with a *kpk_2907*-containing plasmid resulted in a complete recovery of cytoplasmic fumarate reductase activity. KPK_2907 produced in *Escherichia coli* cells contains 1 mol/mol each of covalently bound FMN, noncovalently bound FMN and noncovalently bound FAD. Lesion in the ApbE1 gene in *K. pneumoniae* resulted in inactive Na^+-NQR, but cytoplasmic fumarate reductase activity remained unchanged. On the contrary, lesion in the ApbE2 gene abolished the fumarate reductase but not the Na^+-NQR activity. Both activities could be restored by transformation of the ApbE1- or ApbE2-deficient *K. pneumoniae* strains with plasmids containing the *Vibrio cholerae apb*E gene with or without the periplasm-directing signal sequence, respectively. Our data thus indicate that ApbE1 and ApbE2 bind FMN to Na^+-NQR and fumarate reductase, respectively, and that, contrary to the presently accepted view, the FMN residues are on the periplasmic side of Na^+-NQR. A new, "electron loop" mechanism is proposed for Na^+-NQR, involving an electroneutral Na^+/electron symport. This article is part of a Special Issue entitled: 18th European Bioenergetic Conference.

1. Introduction

Na^+-translocating NADH:quinone oxidoreductase (Na^+-NQR) [1] and related proteins such as Na^+-dependent NADH:ferredoxin oxidoreductase (RNF complex) [2], regulator of NO reductase transcription (NosR) [3] and urocanate reductase (UrdA) [4] contain catalytically essential FMN residues connected by a phosphoester bond through a Thr residue. This post-translational modification is catalyzed by a Mg^{2+}-dependent flavin transferase (ApbE) using FAD as substrate [5]. In *Salmonella enterica*, ApbE is a lipoprotein anchored to the periplasmic side of the inner membrane, and the periplasmic location is essential for the physiological role of ApbE in this bacterium [6]. Homologs of ApbE are widely distributed among bacteria [5].

Na^+-NQR is a redox-driven sodium pump that generates a transmembrane electrochemical Na^+ potential ($\Delta\bar{\mu}_{Na^+}$) [7] and operates in the respiratory chain of various bacteria, including several pathogenic microorganisms [8,9]. Na^+-NQR consists of six subunits (NqrA–F) [10] encoded by the six genes of the *nqr* operon [11,12]. Two covalently bound FMN residues are found in subunits NqrB and NqrC [1,8]. In addition, Na^+-NQR contains a [2Fe–2S] cluster [13,14], noncovalently bound FAD [15,16], riboflavin (Rf) [17], and one tightly bound ubiquinone-8 (UQ_8) [8,16]. FAD and the [2Fe–2S] cluster are localized in subunit NqrF [11,18], whereas riboflavin is found in subunit NqrB [19] and ubiquinone headgroup is located in NqrA [20]. The positions of the prosthetic groups in the electron-transport pathway were deduced from the kinetics of the reduction of wild type [13,21] and

Abbreviations: DCPIP, 2,6-dichlorophenolindophenol; $dNAD^+$ and dNADH, oxidized and reduced nicotinamide hypoxanthine dinucleotide; Na^+-NQR, Na^+-translocating NADH:quinone oxidoreductase; Rf, riboflavin; RNF, Na^+-dependent NADH:ferredoxin oxidoreductase; UQ_8, ubiquinone-8; $\Delta\mu$ Na +, transmembrane electrochemical Na^+ potential

☆ This article is part of a Special Issue entitled: 18th European Bioenergetic Conference.

* Corresponding author at: Department of Molecular Energetics of Microorganisms, Belozersky Institute of Physico-Chemical Biology, Lomonosov Moscow State University, Moscow 119992, Russia. Tel.: +7 495 930 0086; fax: +7 495 939 0338.
E-mail address: bogachev@belozersky.msu.ru (A.V. Bogachev).

0005-2728/$ – see front matter © 2013 Elsevier B.V. All rights reserved.
http://dx.doi.org/10.1016/j.bbabio.2013.12.006

mutant Na^+-NQR lacking FAD, FMN_{NqrB}, FMN_{NqrC} or the [2Fe–2S] cluster [22,23]. The following sequence of electron transport in Na^+-NQR was thus established [7,23]:

$$NADH \rightarrow FAD \rightarrow [2Fe-2S] \xrightarrow{Na^+} FMN_{NqrC} \rightarrow FMN_{NqrB} \rightarrow Rf \rightarrow UQ_8. \quad \text{(Scheme 1)}$$

It should be noted that this scheme may be incomplete as pulsed EPR data showed only weak dipole–dipole interactions between the reduced [2Fe–2S] cluster and NqrC and NqrB flavosemiquinones [24]. Some yet unrecognized redox group(s) may therefore be involved between the [2Fe–2S] cluster and the FMN residues to allow rapid electron transfer between these centers. The rate of electron transport from the [2Fe–2S] cluster to FMN_{NqrC} was found to be strongly activated by sodium ions [21,22]. The apparent binding constants derived from the effects of Na^+ on FMN_{NqrC} and FMN_{NqrB} reduction by NADH and steady-state NADH:ubiquinone conversion are very similar [21]. This finding is consistent with electron transfer from [2Fe–2S] to FMN_{NqrC} being a rate-limiting step coupled with Na^+ pumping [21,23,25].

It is generally believed that the covalently bound FMN residues are localized in the cytoplasmically oriented regions of NqrB and NqrC [26]. However, this view contradicts the periplasmic location of the ApbE enzyme [6] that attaches FMN to Na^+-NQR [5]. To solve this conundrum, we characterize here both ApbE-like proteins of *Klebsiella pneumoniae* with respect to their targets and cellular localization. The results of this study force reconsideration of the currently accepted membrane topology of the Na^+-NQR complex.

2. Materials and methods

2.1. Bacterial strains, growth, and media composition

The bacterial strains used in this study are listed in Table 1. *Escherichia coli* and *K. pneumoniae* cells were routinely grown in LB medium at 37 °C. For measurements of fumarate reductase activities, *K. pneumoniae* cells were grown anaerobically at 37 °C in M9 medium supplemented with 0.2% (w/v) glucose, 0.05% (w/v) yeast extract, and 25 mM sodium fumarate. The media used to grow *K. pneumoniae* cells contained ampicillin at 150 μg/ml, tetracycline at 3.3 μg/ml, 100 μg/ml kanamycin and 40 μg/ml chloramphenicol. The concentrations of the antibiotics used for *E. coli* were 100, 10, 50, and 20 μg/ml, respectively.

2.2. Construction of expression vectors

A C-terminal 6× His-tagged KPK_2907 protein expression vector was constructed by amplifying the DNA fragment of *kpk_2907* by PCR with a Tersus PCR kit (Evrogen) and the primers Kpn_FRD_dir and Kpn_FRD_rev (Table 1) using the genomic DNA of *K. pneumoniae* 204 as a template. The resulting 2790-bp fragment was cloned into the pBAD-TOPO® vector (Invitrogen), yielding the $pBAD\_FRD_{Kpn}3$ plasmid.

An expression vector for the full-length ApbE protein from *Vibrio cholerae* was constructed by amplifying the DNA fragment of *apb*E by PCR with a Tersus PCR kit and the primers VCLAE_dir and VCLAE_rev (Table 1) using *V. cholerae* genomic DNA as the template. The resulting 2100-bp fragment was cloned into the pAL-TA vector (Evrogen), yielding the pAL_VCLAE2 plasmid. The 462-bp *Bsa*BI-*Kpn*I fragment of this plasmid was used to replace the 353-bp *Nco*I-*Kpn*I fragment in the pB_CM1 vector [5]. The resulting plasmid pB_LAE9 contains the *apb*E gene from *V. cholerae* under the control of an arabinose-inducible promoter (*ara*BAD).

2.3. Construction of a KPK_2907-deficient K. pneumoniae strain

A kanamycin-resistance cassette was inserted into the *Eco*RI site of the *kpk_2907* gene in $pBAD\_FRD_{Kpn}3$, and a Km-containing plasmid ($pB\_FRD_{Kpn}\_Km$) bearing the *kpk_2907* gene together with the unidirectionally transcribed kanamycin-resistance cassette was selected. The *kpk_2907*::Km fragment from $pB\_FRD_{Kpn}\_Km$ was subcloned into the suicide vector pKNOCK-Tc, resulting in pKn_FRD::Km. This plasmid was transferred into the *K. pneumoniae* KNU210 (*nuo*B::Cm) strain [27] via conjugation using *E. coli* SM10λpir as the donor, and a Tc^S Km^R Cm^R

Table 1
Bacterial strains, plasmids, and primers used in this study.

	Relevant details	Reference or source
Strain		
K. pneumoniae 204	Wild type	[27]
K. pneumoniae KNU210	*nuo*B::Cm, Rf^R Cm^R	[27]
K. pneumoniae KNUAE11	*nuo*B::Cm, *apb*E1::Km, Rf^R Cm^R Km^R	[5]
K. pneumoniae 503	*nuo*B::Cm, *apb*E2::Km, Rf^R Cm^R Km^R	This study
K. pneumoniae 307	*nuo*B::Cm, *kpk_2907*::Km, Rf^R Cm^R Km^R	This study
E. coli Sm10 λpir	*thi thr leu ton*A *lacY sup*E *rec*A::RP4-2-Tc::Mu, Km^R	[53]
E. coli XL1-Blue	*rec*A1 *end*A1 *gyr*A96 *thi*-1 *hsd*R17 *sup*E44 *rel*A1 *lac* [F′ *pro*AB *lacI*^{q}ZΔM15 Tn10], Tc^R	Stratagene
Plasmid		
pKNOCK-Tc	Mobilizable suicide vector; Tc^R	[54]
pAL-TA	PCR products TA-cloning vector; Ap^R	Evrogen
pBAD-TOPO	Recombinant protein expression vector, Ap^R	Invitrogen
pBAD	Recombinant protein expression vector, Ap^R	Invitrogen
pB_LAE9	pBAD bearing the full length *apb*E gene of *V. cholerae*, Ap^R	This study
pB_CM1	pBAD bearing a truncated *apb*E gene of *V. cholerae* without nucleotides 1–48, with C17M substitution, *pUC ori*, Ap^R	[5]
pΔhis3	pBAD bearing a truncated *apb*E gene of *V. cholerae* without nucleotides 1–48, with C17M substitution, *p15A ori*, Cm^R	[5]
$pBAD\_FRD_{Kpn}3$	pBAD-TOPO bearing the *kpk_2907* gene of *K. pneumoniae* and C-terminal 6×His tag, Ap^R	This study

Primer	Sequence (5′–3′)[a]
Kpn_FRD_dir	GagGaaTAACTTATGACCAGTAACGAACGTA
Kpn_FRD_rev	ggATCCTCTGGCACGTTTCGC
VCLAE_dir	GACTCCGCCGCCAAATAATC
VCLAE_rev	GGCAGCGAAAAAGCAGTCCA
Kpn_ApbE2_dir	CTTCAACGAGATGGAGACCCG
Kpn_ApbE2_rev	CTGGTGCTGCTGGATGTCTAC

[a] The nucleotides substituted in mutagenesis experiments are designated by lower case letters.

phenotype clone (*K. pneumoniae* 307 *nuo*B::Cm, *kpk_2907*::Km) characteristic of a double-crossover—introduced mutation was selected.

2.4. Construction of an ApbE2-deficient K. pneumoniae strain

A DNA fragment containing the *apb*E2 gene was amplified by PCR with *Taq* polymerase and primers Kpn_ApbE2_dir and Kpn_ApbE2_rev (Table 1) using *K. pneumoniae* 204 genomic DNA as a template. The amplified 2097-bp fragment was cloned into the pAL-TA vector, resulting in the pAL_ApbE2_6 plasmid. A kanamycin-resistance cassette was inserted into the *Age*I site of the *apb*E2 gene in pAL_ApbE2_6, and a Km-containing plasmid (pALAE2_Km1) bearing the *apb*E2 gene together with the unidirectionally transcribing kanamycin-resistance cassette was selected. The *apb*E2::Km fragment from pALAE2_Km1 was subcloned into the suicide vector pKNOCK-Tc, resulting in pKn_AE2::Km1. This plasmid was transferred into the *K. pneumoniae* KNU210 (*nuo*B::Cm) strain via conjugation using *E. coli* SM10λpir as the donor, and a Tc^S Km^R Cm^R phenotype clone (*K. pneumoniae* 503, *nuo*B::Cm, *apb*E2::Km) characteristic of a double-crossover—introduced mutation was selected. Proper localization of the mutations in the *K. pneumoniae* chromosome was verified by PCR analysis.

2.5. Subcellular fractionation of K. pneumoniae cells

K. pneumoniae cells were harvested by centrifugation (10,000 *g*, 10 min) and washed with medium 1 (100 mM KCl, 10 mM Tris–HCl, 5 mM $MgSO_4$, pH 8.0). The periplasmic fraction was obtained by a Polymyxin B treatment [28]. The cell pellet was suspended in ice-cold medium 2 (100 mM KCl, 20 mM Tris/HEPES (pH 8.0), 5 mM $MgSO_4$) supplemented with Polymyxin B (10,000 units/ml). This mixture was gently stirred in an ice bath for 10 min. The Polymyxin B-treated cells were removed by centrifugation (10,000 *g*, 10 min). The supernatant represented the periplasmic fraction of *K. pneumoniae* cells. Control experiments showed that this treatment resulted in a >90% release of periplasmic proteins (estimated by measuring β-lactamase activity) with ≤1% contamination by cytoplasmic proteins (estimated by measuring malate dehydrogenase activity).

To produce cytoplasmic and membrane fractions, the pelleted Polymyxin B-treated cells were suspended in medium 2 and the suspension was passed through a French press (16,000 psi). Undamaged cells and cell debris were removed by centrifugation at 22,500 *g* (10 min), and the supernatant was further centrifuged at 180,000 *g* (60 min). The supernatant was used as the cytoplasmic fraction. The pellet was then washed with medium 2, suspended in the same medium, and used as the membrane fraction. Protein concentration was determined by a bicinchoninic acid method [29] using bovine serum albumin as a standard.

2.6. Determination of enzymatic activities

Fumarate reductase activity was determined spectrophotometrically by following the oxidation of reduced methyl viologen (ε_{606} = 13.7 mM^{-1} cm^{-1} [30]). The assay was performed in a 3.2 ml anaerobic cuvette. The standard assay mixture contained 100 mM KCl, 20 mM Tris/HEPES (pH 8.0), 5 mM $MgSO_4$, 1 mM fumarate, and 1 mM methyl viologen reduced with sodium dithionite until an absorbance of about 1.5 at 606 nm was obtained.

Succinate dehydrogenase activity was measured at 600 nm by following the reduction of 2,6-dichlorophenolindophenol (DCPIP, ε_{600} = 22 mM^{-1} cm^{-1}) [31]. The assay mixture contained 100 mM KCl, 20 mM Tris/HEPES (pH 8.0), 5 mM $MgSO_4$, 2 mM succinate, 2 mM phenazine methosulfate, and 25 μM DCPIP.

Na^+-NQR activity of membrane vesicles isolated from *K. pneumoniae* strains with Δ*nuo*B genetic background was measured at 340 nm by following the sodium-stimulated component of oxidation of the potassium salt of dNADH (ε_{340} = 6.22 mM^{-1} cm^{-1}). Na^+-NQR is the sole dNADH-oxidizing complex of the respiratory chain in these *K. pneumoniae* strains owing to disruption of the *nuo*B gene encoding a subunit of H^+-translocating NADH:quinone oxidoreductase (NDH-1) [27]. The other NADH:quinone oxidoreductase (NDH-2) of *K. pneumoniae* oxidizes NADH but not dNADH, whereas Na^+-NQR acts on both substrates [27,32]. The reaction medium contained 100 mM KCl, 20 mM Tris/HEPES (pH 8.0), 5 mM $MgSO_4$, and 120 μM K-dNADH. To determine Na^+-stimulation of the activity, 25 mM NaCl was added to the reaction mixture.

The assays were performed at 25 °C and absorbance measurements were carried out using a Hitachi 557 spectrophotometer. One unit of enzyme activity was defined as the amount of enzyme catalyzing oxidation of 2 μmol of methyl viologen, 2 μmol of DCPIP or 1 μmol of dNADH per min.

2.7. Synthesis of the potassium salt of dNADH

Only sodium salts of dNADH are commercially available. K-dNADH was produced by reduction of $dNAD^+$ upon incubation with ethanol, alcohol dehydrogenase, and semicarbazide [33,34]. The dNADH produced was precipitated by barium acetate/ethanol treatment [34]. The potassium salt of dNADH was obtained by treatment of the produced Ba-dNADH with K_2SO_4.

2.8. Isolation of recombinant 6× His-tagged KPK_2907 protein

For *kpk_2907* induction, *E. coli* cells bearing the pBAD_FRD_{Kpn}3 and pΔhis3 [5] plasmids were grown at 32 °C to mid-exponential phase (A_{600} = 0.3–0.4), after which the growth medium was supplemented with 0.2% (w/v) L-arabinose and the cells were grown for additional 3 h. The cells were harvested by centrifugation (10,000 *g*, 10 min) and washed twice with medium containing 300 mM NaCl, 10 mM Tris–HCl, and 5 mM $MgSO_4$ (pH 8.0). The cell pellet was suspended in medium containing 300 mM NaCl, 20 mM Tris–HCl, 5 mM $MgSO_4$, 1 mM phenylmethylsulfonyl fluoride, and 5 mM imidazole–HCl (pH 8.0), and the suspension was passed twice through a French press (16,000 psi). Cell debris and membrane vesicles were removed by centrifugation at 180,000 *g* (60 min). The KPK_2907-6His protein was purified from the supernatant using affinity chromatography. This was accomplished by loading the supernatant onto a Ni-NTA column equilibrated with solution A containing 300 mM NaCl, 10 mM Tris–HCl, and 5 mM imidazole–HCl (pH 8.0); washing the column first with solution A containing 10 mM imidazole–HCl and then with solution A containing 20 mM imidazole–HCl; and eluting KPK_2907-6His with solution A containing 100 mM imidazole–HCl. The protein obtained was concentrated and kept frozen at −80 °C until use.

2.9. Extraction and identification of flavins in KPK_2907

Covalently and noncovalently bound flavins in the KPK_2907-6His protein were assayed as described by Casutt et al. [35]. The protein (3 mg) was precipitated with 7.5% (v/v) trifluoroacetic acid, sedimented by centrifugation, and washed with water (0 °C). The supernatants were combined, neutralized by adding 0.8 M K_2HPO_4, and passed through a Microcon YM-10 centrifugal filter (Millipore). The filtrate was used for determination of noncovalently bound flavins. Covalently bound flavins were released from the protein pellet by alkaline hydrolysis. To this end, an ice-cold 0.5 M LiOH solution (0.2 ml) was added to the pellet and the mixture was vortexed and incubated on ice for 24 h. After the incubation, the suspension was neutralized by adding 1 M MES and passed through a Microcon YM-10 centrifugal filter. The filtrates obtained were subjected to reverse-phase HPLC using a Prontosil 120-5 C18 column (75 × 2 mm). A linear gradient of methanol (ranging from 10% to 70% v/v, 25 min) in 5 mM MES–Tris (pH 6.0) with a flow rate of 0.1 ml/min was used. Flavins were detected at 360 nm.

2.10. Electrophoresis

SDS-PAGE was performed using 10% (w/v) polyacrylamide gels [36]. Covalently bound flavins were detected by photographing gels under UV illumination with a Gel-Imager2 gel documentation system using a SYBR Green emission filter.

3. Results

3.1. Bioinformatic analysis of K. pneumonia genome

The *K. pneumoniae* genome [37] contains genes for two ApbE-type proteins—ApbE1 and ApbE2 [5]. Despite only moderate similarities in their deduced amino acid sequences (32% identity), they contain most of the residues involved in FAD binding identified in the crystal structure of *S. enterica* ApbE [38]. These residues are also found in *V. cholerae* ApbE, the only ApbE protein for which flavin transferase activity has been experimentally demonstrated [5]. The two ApbE proteins of *K. pneumoniae* are thus also expected to act as flavin transferases. One important difference between these putative flavin transferases is that the predicted ApbE1 sequence contains a 20-residue N-terminal extension (MDMTFFRAALLGACVLLSGC), which was identified by LipoP 1.0 server [39] as a periplasm-addressing signal for bacterial lipoproteins. This extension or any other signal peptide is absent in ApbE2 (Fig. 1). Furthermore, ApbE2 lacks any transmembrane α-helix and therefore should be a cytoplasmic protein.

Adjacent to the *apb*E2 gene in the *K. pneumoniae* chromosome is a gene encoding a 925-residue protein KPK_2907, formed by three domains: OYE_like_FMN (Pfam: PF00724), FMN_bind (Pfam: PF04205), and FAD_binding_2 (Pfam: PF00890) (Fig. 2A) [40]. Intriguingly, the FMN_bind domain contains a Dxx(s/t)gAT* motif (lower case letters indicate preferred but not strictly conserved residues, *x* is any residue), characteristic of proteins to which FMN is covalently attached via a Thr residue (marked with an asterisk) [5]. The C-terminal FAD_binding_2 domain is homologous to the FAD-binding domain of fumarate reductases (succinate dehydrogenases) and contains all the amino acid residues that are critical for these catalytic activities (Fig. 2B). Noteworthy, in KPK_2907, this domain lacks a characteristic His residue to which FAD is covalently attached via an 8α-*N*-histidyl–FAD bond in membrane-bound fumarate reductases (succinate dehydrogenases) (Fig. 2B) and may thus bind FAD noncovalently. The N-terminal OYE_like_FMN domain is homologous to "old yellow enzyme"; thus, an NAD(P)H-dehydrogenase activity could be expected for this domain. Importantly, the N-terminus of KPK_2907 bears no signal sequence that would direct it outside the cytoplasm. Based on this analysis, KPK_2907 could be tentatively classified as a cytoplasmic fumarate reductase (succinate dehydrogenase) that uses a covalently bound FMN residue for catalysis and is thus a target for ApbE2.

3.2. Isolation and characterization of KPK_2907

The *kpk_2907* gene was amplified from *K. pneumoniae* genomic DNA and cloned into the expression vector pBAD-TOPO, containing an arabinose-inducible promoter (*ara*BAD) and an insert for a His_6 tag at the C-terminus of the expressed protein. *E. coli* cells expressing *kpk_2907* did not exhibit cytoplasmic fumarate reductase activity, which could be explained by the inability of *E. coli* to flavinylate foreign proteins [5]. Accordingly, *kpk_2907* expression in *E. coli* in the presence of a plasmid containing the gene encoding *V. cholerae* ApbE devoid of its signal peptide (*Vc*_ApbE′) induced high fumarate reductase activity (5.4 μmol of reduced fumarate/min per mg protein). These data indicated the importance of KPK_2907 flavinylation for its catalytic activity.

The active KPK_2907-6His was isolated from the *E. coli*/pBAD_FRD_{Kpn}3 + pΔhis3 strain as a bright yellow protein by immobilized metal affinity chromatography on Ni-NTA agarose. The protein was detected as a ~95-kDa fluorescent band (99.5 kDa calculated mass) in SDS-polyacrylamide gels (Fig. 3A), confirming the presence of a covalently bound flavin. The absorption spectrum of the isolated protein showed maxima at 369 and 457 nm, characteristic of flavin prosthetic groups (Fig. 3B). The flavin content of KPK_2907-6His could be calculated from these data as 9.3 nmol per mg of protein.

The relative amounts of covalently and noncovalently bound flavins in the recombinant KPK_2907-6His were determined as described by Barquera et al. [17]. The protein was denatured by guanidine hydrochloride and the released noncovalently bound flavins were separated by ultrafiltration. Two thirds (67%) of the total flavin content of KPK_2907-6His was found to be noncovalently bound and nearly one third (27%) was found to be covalently bound (a small amount of the covalently bound flavin was apparently lost because of protein adsorption on the filter). Thus, the ratio of the covalently and noncovalently bound flavins in KPK_2907-6His was about 1:2. This finding is consistent with the sequence data showing the presence of a flavin covalent binding motif in only one of the three flavin-binding domains in KPK_2907.

To identify the flavins present in KPK_2907-6His, the purified protein was precipitated with 7.5% (v/v) trifluoroacetic acid and sedimented by centrifugation. HPLC analysis of the supernatant demonstrated the presence of nearly equal amounts of FAD and FMN (Fig. 3C, upper trace). The covalently bound flavin was extracted from the protein pellet by alkaline treatment as described by Casutt et al. [35]. HPLC analysis of the extract revealed only FMN (Fig. 3C, lower trace). To sum up, active recombinant KPK_2907 contains approximately equal amounts of noncovalently bound FAD, noncovalently bound FMN, and covalently bound FMN.

The isolated KPK_2907-6His demonstrated high fumarate reductase activity (k_{cat} = 540 s^{-1} with reduced methyl viologen as an electron donor) and negligible succinate dehydrogenase activity (0.005 s^{-1}),

```
ApbE1 : MDMTFFRAALLGACVLLSGCDSATTPASPASTATVLDGKTMGTFWRVSVIGVDEAAAEALRAKVQAQLDADDRLLSTWKNDSAL
ApbE2 : ---------------------------MSDNRVYSYSAVLMGSPILLKLYSHDEAIASRVFQLIKRYEE----LLTVNRAESQV

ApbE1 : MRFNHAADTRPWPVSEAVVDIVTLSLRIGAKTHGAMDITVGPLVNLWGFGPDKQPVTTPDAQAIAAAKARTGIQHLQVINQSGR
ApbE2 : MDINHAAGRHPVTVSRPVFQLIQCAKAASMVRDSAFNIAIGPLVKLWRIGFHGHSV--PDAADIRARLALTRPQEVILDETTCS

ApbE1 : QFLQKDIPDLFVDLSTVGEGYAADHIARIMEQEGISRYLVSVGGAIVSRGMNGEGKPWRVAIQKPTDRENAVQAIVDINGHGIS
ApbE2 : VFLQQ--PGMELDLGAIAKGYIADRVRDYLRQQGVEKALINLGGNVHTLG------EWTIGLKKPFADAQALIGSLTINGQSVV

ApbE1 : TSGSYRNYYELDGKRISHVIDPQTGQPITHKLVSVTVIAPTALEADGWDTGLMVLGPEKAQQVVREQGLAVYMIVKEGEGFKTW
ApbE2 : TSGTYERYFEQDGKRWHHILDPRSGYPLDNELDSVTVISTDSLDGDIWTTLLFGLGVEKGCAALRQREDIDAIFWTKNRDI-IL

ApbE1 : MSPQFRTSLVGEKN--------
ApbE2 : SSPQRLRESPLDSGYQVIDCTA
```

Fig. 1. Sequence alignment of the ApbE-like proteins of *K. pneumoniae*, ApbE1 (accession number YP_002237370) and ApbE2 (YP_002238733). Identical residues are shown in boxes.

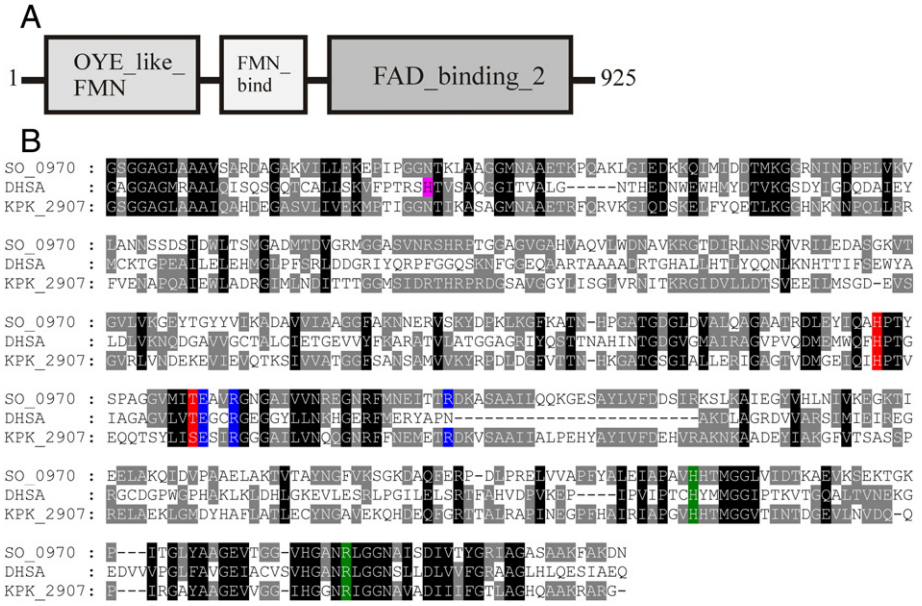

Fig. 2. The structure of *K. pneumoniae* KPK_2907. Panel A: the domain architecture of *K. pneumoniae* KPK_2907. Panel B: sequence alignment of the FAD-binding domain of the periplasmic fumarate reductase from *S. oneidensis* MR-1 (SO_0970, accession number AAN54044), the flavoprotein subunit of the succinate dehydrogenase from *E. coli* (DHSA, accession number ZP_07190469), and the FAD-binding domain of the KPK_2907 protein from *K. pneumoniae* (YP_002238734). Amino acid residues involved in binding the C4 carboxylic group of fumarate are marked in green, residues forming the proton transfer pathway to fumarate are marked in blue, and residues involved in binding the C1 carboxylic group of fumarate are marked in red. The histidine residue that anchors FAD in the succinate dehydrogenase is marked in magenta.

values quite comparable with those for other known soluble fumarate reductases [41,42]. However, contrary to expectation, KPK_2907-6His exhibited no NAD(P)H-dependent fumarate reductase activity. Moreover, prolonged incubation of KPK_2907-6His with NADH or NADPH did not result in protein reduction (data not shown). A likely explanation is that KPK_2907 uses an electron donor other than NAD(P)H in vivo. Alternatively, KPK_2907 could be a bifurcating enzyme that requires ferredoxin or another low potential electron acceptor, beside NAD(P)H and fumarate, for enzymatic activity in vivo [43].

3.3. Cellular localization of KPK_2907

K. pneumoniae cells grown anaerobically in the presence of fumarate were separated into cytoplasmic, periplasmic, and membrane fractions, and their fumarate reductase and succinate dehydrogenase activities were measured (Table 2). The highest level of fumarate reductase (95% of its total cell content) was observed in the cytoplasm, and only 4% of the total activity was found in the membrane fraction. The corresponding specific activities of fumarate reductase in the cytoplasmic and membrane fractions were 2.8 ± 0.1 and 0.39 ± 0.05 units/mg. Small amounts of the enzyme in the periplasmic fraction (1%) apparently resulted from cytoplasmic contamination. Importantly, the membrane fraction exhibited both fumarate reductase and succinate dehydrogenase activities, whereas the cytoplasmic fraction showed only the former activity. These findings agree with the reported data [42] showing that soluble fumarate reductases are generally unidirectional catalysts, whereas membrane-bound fumarate reductases/succinate dehydrogenases catalyze fumarate-to-succinate interconversion in both directions. The low fumarate reductase activity in the membrane fraction therefore cannot be fully explained by cytoplasmic contamination. Hence, the *K. pneumoniae* cells grown anaerobically in the presence of fumarate contain at least two enzymes with fumarate reductase activity—one in the cytoplasm and the other in the membrane.

To clarify the role of KPK_2907 in the fumarate reductase activity of *K. pneumoniae* cells, we prepared a mutant strain of the bacterium with inactivated *kpk_2907* gene. This strain lacked cytoplasmic fumarate reductase activity, whereas both activities in the membrane fraction were only slightly affected (Table 2). Complementation of the

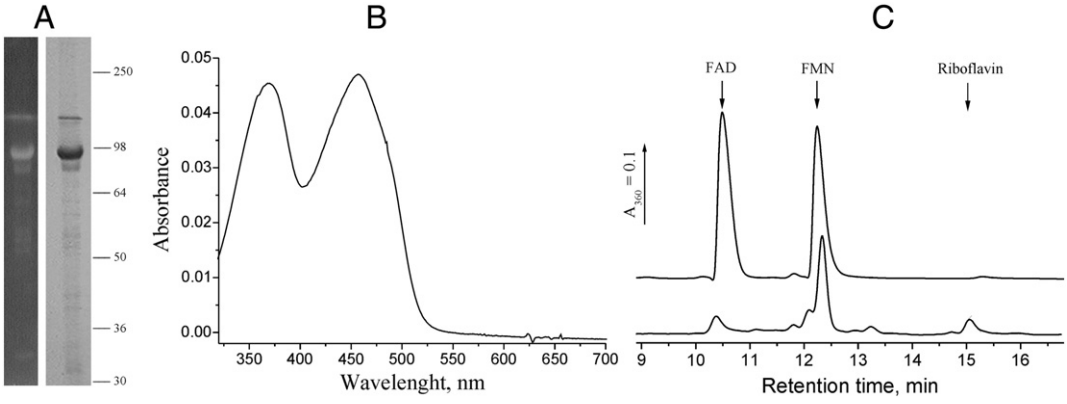

Fig. 3. Characterization of the recombinant protein KPK-2907-6His purified from the *E. coli*/pBAD_FRD$_{Kpn}$3 + pΔhis3 strain. (A) SDS-PAGE analysis. Left: unstained gel under UV illumination. The major fluorescent band corresponds to flavin-bound KPK_2907-6His. Right: Coomassie Blue-stained gel. The bars with numbers indicate the positions and molecular masses (in kDa) of marker proteins. (B) Electronic absorption spectrum. (C) HPLC separation of noncovalently bound flavins (upper trace) and covalently bound flavins (lower trace) released from KPK_2907-6His. Retention times for FAD, FMN, and riboflavin are indicated by arrows.

Table 2
Fumarate reductase/succinate dehydrogenase activities of cellular fractions prepared from two *K. pneumoniae* strains. Cell amounts equivalent to 13 mg of cellular protein were used for each strain. The results of a typical experiment are shown.

Strain	Activity (unit)		
	Membrane	Periplasm	Cytoplasm
K. pneumoniae KNU 210 (Δ*nuo*)	1.2/0.024	0.26/<0.001	28/<0.001
K. pneumoniae 307 (Δ*nuo* Δ*kpk_2907*)	0.5/0.021	<0.01/<0.001	<0.01/<0.001

K. pneumoniae 307 (Δ*kpk_2907*) strain with the *kpk_2907*-containing plasmid pBAD_FRD$_{Kpn}$3 resulted in a complete recovery of cytoplasmic fumarate reductase activity (specific activity of 4.2 units/mg versus 2.8 units/mg in wild-type cells). Taken together, these finding indicated that the cytoplasmically localized fumarate reductase activity is associated with the KPK_2907 protein in *K. pneumoniae*.

3.4. Flavinylation of KPK_2907 and Na^+-NQR subunits in *K. pneumoniae* cells

Since both the membrane-bound Na^+-NQR and the cytoplasmic KPK_2907 contain covalently bound FMN residues, it was of interest to determine which of the two ApbE-like proteins (ApbE1 and ApbE2) is responsible for their modification in *K. pneumoniae*. As Table 3 makes clear, *apb*E1 lesion resulted in a complete loss of Na^+-NQR activity, whereas *apb*E2 lesion had no effect on it. The effects on KPK_2907 activity were the opposite: no effect of the *apb*E1 mutation and complete inactivation by the *apb*E2 lesion. A straightforward inference is that ApbE1 is essential for Na^+-NQR flavinylation while ApbE2 catalyzes this reaction with KPK_2907.

The selectivity of *K. pneumoniae* ApbE1 and ApbE2 for Na^+-NQR and KPK_2907, respectively, may result from their intrinsic specificities or differential cellular localization of the modifying enzymes and/or their targets. To choose between these alternatives, we transformed *apb*E1- and *apb*E2-mutated *K. pneumoniae* cells with plasmids containing the *V. cholerae apb*E gene. *V. cholerae* ApbE was chosen for the complementation because it is the only ApbE-type flavin transferase in the host bacterium and can use proteins from different organisms as targets [5]. This protein contains an N-terminal signal peptide, presumably directing it to the periplasm (Fig. 4). One of the plasmids (pB_LAE9) used to transform *K. pneumoniae* cells contained the complete *V. cholerae apb*E gene, while the second (pB_CM1) contained a truncated *V. cholerae apb*E gene devoid of its signal sequence. The former plasmid should produce periplasmically localized ApbE, whereas the latter should yield cytoplasmic ApbE.

As shown in Table 3, the effects of the plasmids on Na^+-NQR and fumarate reductase activities were in opposition. The plasmid containing wild type *Vc_apb*E did not complement fumarate reductase activity in *apb*E2-mutated *K. pneumoniae* but did complement Na^+-NQR activity in the *apb*E1-mutated cells. In contrast, the plasmid containing truncated *apb*E′ fully complemented fumarate reductase activity in the *apb*E2-mutated cells but was ineffective with Na^+-NQR activity in the *apb*E1-mutated cells. These results consistently showed that cytoplasmically localized KPK_2907 fumarate reductase requires cytoplasmic ApbE enzyme for flavinylation. Another inference is that flavinylation of Na^+-NQR occurs in the periplasmic space. These findings provide a rationale for the presence of two forms of the ApbE enzyme with different localizations in *K. pneumoniae*.

4. Discussion

The results reported above indicate that the high fumarate reductase activity detected in the cytoplasm of the *K. pneumoniae* cells grown anaerobically in the presence of fumarate is associated with the cytoplasmic protein KPK_2907. This enzyme contains three flavin prosthetic groups and has a unique domain composition not found previously in other fumarate reductases. Another unusual property of KPK_2907 is that FMN is attached covalently to this cytoplasmic protein. In most known cases, covalent attachment of FMN is associated with its periplasmic location. Despite its apparent uniqueness, the KPK_2907 type of fumarate reductase may be widespread among bacteria because its homologs are present in microorganisms belonging to the genera *Klebsiella*, *Erwinia*, *Enterobacter*, *Photobacterium*, *Vibrio*, *Staphylococcus*, *Streptococcus*, *Enterococcus* and others, including pathogenic *Staphylococcus aureus*, *Staphylococcus epidermidis* and *Streptococcus uberis* species.

Although not directly demonstrated in this work, FMN apparently forms a phosphoester bond with Thr-447 in KPK_2907. This contention is based on the findings that the KPK_2907 sequence contains a specific motif for this kind of post-translational modification [5] and that KPK_2907 is active only when its gene is co-expressed in *E. coli* with the gene encoding the specific flavin transferase (ApbE) capable of such a modification. Of the two ApbE enzymes present in *K. pneumoniae*, only the cytoplasmic form (ApbE2) can modify KPK_2907, consistent with the cytoplasmic localization of KPK_2907. The periplasmic form (Vc_ApbE) can modify KPK_2907 in vivo only when redirected to the cytoplasm by removing the signal peptide.

In contrast, Na^+-NQR is flavinylated only by the periplasmic ApbE and the reaction does not proceed in cells containing the same ApbE but without the signal peptide. Our data thus convincingly demonstrate that essential flavin groups are attached to Na^+-NQR subunits in the periplasm. As post-translational modification usually succeeds protein integration into the membrane, our findings suggest a periplasmic orientation of the flavin-binding domains of NqrC and NqrB in mature Na^+-NQR. This inference is supported by a similar topology of their paralogous subunits (RnfD and RnfG) in the related RNF complex [2]. It should be noted that the lengthy ribosyl bridge may allow the hydrophobic isoalloxazine ring of FMN$_{NqrB}$ to be submerged into the membrane portion of the subunit from the periplasmic side. Such an arrangement is, however, unlikely in the case of the NqrC subunit because its truncated form, devoid of the transmembrane α-helix, is a water-soluble flavoprotein with spectral and redox properties [5] similar to those of the full-size NqrC in the complete Na^+-NQR complex [44].

The periplasmic orientation of FMN has important implications for the transport reactions catalyzed by Na^+-NQR. It was earlier suggested that Na^+-NQR operates by a mechanism similar to that of Complex I. According to that mechanism, all the prosthetic groups of Na^+-NQR are located on the cytoplasmic side of the membrane and electron transport between these groups is coupled to transmembrane Na^+ transport via long-range conformational changes [23,24]. Given the known sequence of the redox events (Scheme 1) and that it should start and end on the cytoplasmic side of the membrane [26], electrons should cross the membrane twice on the way from NADH to ubiquinone to reach the flavins on the periplasmic side. Such an "electron-loop" mechanism, depicted in Fig. 5, is consistent with the weak dipole–dipole interactions between the reduced [2Fe–2S] cluster and NqrC and NqrB flavosemiquinones [24], as these groups are located on the different

```
Vc_ApbE    MRNWLVALASLLLLAGCEKPAEQVHLS...
Vc_ApbE'               MEKPAEQVHLS...
```

Fig. 4. N-terminal sequences of authentic (*Vc*_ApbE) and truncated (*Vc*_ApbE′) *V. cholerae* ApbE proteins. P-, H-, and L-boxes of the signal peptide are shown as blue, gray and yellow boxes, respectively; the Cys residue through which fatty acids are attached is shown in red.

Table 3
The effects of mutations in *apb*E1 and *apb*E2 on the activities of membrane-bound Na^+-NQR and cytoplasmic fumarate reductase in *K. pneumoniae* strains, as estimated from Na^+-stimulated dNADH oxidation and fumarate reduction, respectively, and their complementation with plasmids carrying *V. cholerae apb*E or *apb*E′.

K. pneumoniae strain	Plasmid (encoded *V. cholerae* protein)	Activity (unit/mg)	
		Na^+-NQR	KPK_2907
Wild type	None	0.11 ± 0.03	2.8 ± 0.1
Δ*apb*E1	None	<0.01	2.7 ± 0.1
Δ*apb*E2	None	0.12 ± 0.02	<0.01
Δ*apb*E1	pB_LAE9 (*Vc*_ApbE)	0.11 ± 0.03	n.d.[a]
Δ*apb*E1	pB_CM1 (*Vc*_ApbE′)	<0.01	n.d.
Δ*apb*E2	pB_LAE9 (*Vc*_ApbE)	n.d.	<0.01
Δ*apb*E2	pB_CM1 (*Vc*_ApbE′)	n.d.	2.6 ± 0.1

[a] n.d., not determined.

sides of the membrane. To ensure efficient electron transfer, redox-active groups should be separated by <14 Å [45]. Hence, at least two more such groups are required in the membrane portion between the [2Fe–2S] cluster and FMN_{NqrC}. Although the nature of these groups is currently unknown, the likely candidates are the four membrane-embedded Cys residues of NqrD and NqrE, earlier suggested to take part in electron transfer [46]. Possible involvement of these residues in redox activity is supported by their being virtually invariant residues that are replaced by only selenocysteines in the Na^+-NQR of several marine bacteria [47,48].

Na^+ translocation through Na^+-NQR apparently occurs during electron transfer from the [2Fe–2S] cluster to FMN_{NqrC} [7,22]. The "electron loop" mechanism in Fig. 5 has the obvious merit of permitting a smaller charge separation during the transport reactions because Na^+ is co-transported with an electron. As the $Na^+/\bar{e}$ stoichiometry is 1 in Na^+-NQR [49], such an electroneutral symport should produce only

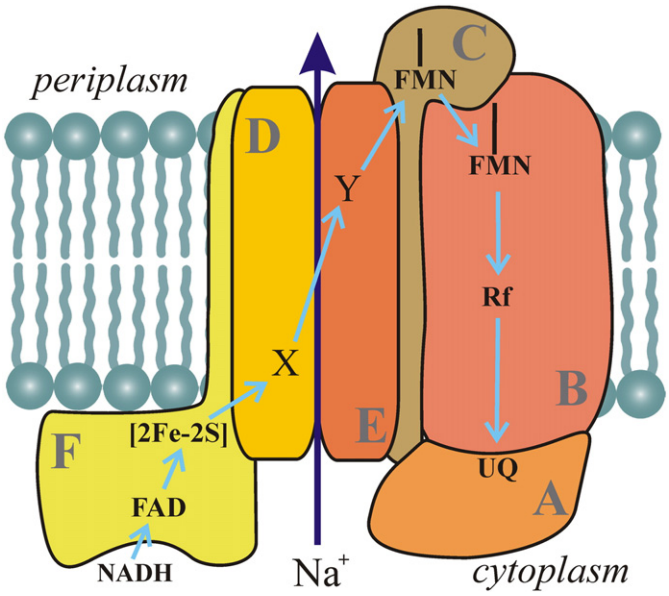

Fig. 5. Topology and proposed reaction mechanism of Na^+-NQR in the bacterial membrane. Electron and Na^+ pathways are shown with gray-blue and violet arrows, respectively. NqrA–F subunits are designated by corresponding capital letters, Rf denotes riboflavin, UQ is ubiquinone, X and Y are putative redox-active prosthetic groups between the distant [2Fe–2S] cluster and FMN_{NqrC}. The shown membrane topology of the Na^+-NQR subunits is entirely based on the literature data [26]: NqrA is a cytoplasmically localized water soluble subunit; NqrB, NqrD and NqrE are formed by 8, 6 and 6 membrane-embedded α-helices, respectively; NqrC and NqrF each have only one transmembrane α-helix and large solution oriented parts. The assignment of the redox-active groups to different subunits [23] and the order of the redox events [7,23], except for X and Y, is also based on literature data. Two new features of this scheme, directly following from our data, are the placement of FMN_{NqrB} and FMN_{NqrC} (and their corresponding binding domains) on the periplasmic side and addition of X and Y. The rate of electron transport from the [2Fe–2S] cluster to FMN_{NqrC} is known to be strongly activated by sodium ions [21,22] indicating that some step in between is coupled with Na^+ pumping.

ΔpNa, whereas Δψ generation will occur upon electron transfer from FMN_{NqrC} to ubiquinone. This scheme is supported by single-turnover data showing the role of riboflavin oxidoreduction in Δψ generation [50]. Separating the process of $\Delta\bar{\mu}_{Na^+}$ generation into two successive steps should facilitate Na^+-NQR catalysis by reducing its activation barrier.

Covalent bonding of flavins is usually associated with the need to change their redox properties in proteins [51]. This explanation is likely in cases where flavins are attached via the isoalloxazine ring. In the NqrB and NqrC subunits of Na^+-NQR, the RnfD and RnfG subunits of the RNF complex [2], regulator of NO reductase transcription NosR [3], and urocanate reductase UrdA [4], the FMN residue is attached via the phosphate group, i.e., at a distance from the isoalloxazine ring. Therefore, an effect of such covalent bonding on flavin redox properties seems unlikely in these proteins. Instead, our data on the periplasmic location of the bound FMN residues suggest that the covalent bonding simply helps to prevent cofactor loss to the external medium. A similar interpretation of the covalent bonding of a heme group was suggested for cytochrome *c* [52].

In summary, we have identified a novel cytoplasmic fumarate reductase and flavin transferase in *K. pneumoniae* and demonstrated that FMN residues are attached to Na^+-NQR on its periplasmic side. Based on the latter finding, an "electron loop" mechanism is proposed for coupling the transport reactions in Na^+-NQR.

Acknowledgements

This work was supported by the Russian Foundation for Basic Research (project numbers 13-04-00332 and 12-04-01002).

References

[1] M. Hayashi, Y. Nakayama, M. Yasui, M. Maeda, K. Furuishi, T. Unemoto, FMN is covalently attached to a threonine residue in the NqrB and NqrC subunits of Na^+-translocating NADH-quinone reductase from *Vibrio alginolyticus*, FEBS Lett. 488 (2001) 5–8.
[2] J. Backiel, O. Juárez, D.V. Zagorevski, Z. Wang, M.J. Nilges, B. Barquera, Covalent binding of flavins to RnfG and RnfD in the Rnf complex from *Vibrio cholerae*, Biochemistry 47 (2008) 11273–11284.
[3] P. Wunsch, W.G. Zumft, Functional domains of NosR, a novel transmembrane iron–sulfur flavoprotein necessary for nitrous oxide respiration, J. Bacteriol. 187 (2005) 1992–2001.
[4] A.V. Bogachev, Y.V. Bertsova, D.A. Bloch, M.I. Verkhovsky, Urocanate reductase: identification of a novel anaerobic respiratory pathway in *Shewanella oneidensis* MR-1, Mol. Microbiol. 86 (2012) 1452–1463.
[5] Y.V. Bertsova, M.S. Fadeeva, V.A. Kostyrko, M.V. Serebryakova, A.A. Baykov, A.V. Bogachev, Alternative pyrimidine biosynthesis protein ApbE is a flavin transferase catalyzing covalent attachment of FMN to a threonine residue in bacterial flavoproteins, J. Biol. Chem. 288 (2013) 14276–14286.
[6] B.J. Beck, D.M. Downs, A periplasmic location is essential for the role of the ApbE lipoprotein in thiamine synthesis in *Salmonella typhimurium*, J. Bacteriol. 181 (1999) 7285–7290.
[7] M.I. Verkhovsky, A.V. Bogachev, Sodium-translocating NADH:quinone oxidoreductase as a redox-driven ion pump, Biochim. Biophys. Acta 1797 (2010) 738–746.
[8] W. Zhou, Y.V. Bertsova, B. Feng, P. Tsatsos, M.L. Verkhovskaya, R.B. Gennis, A.V. Bogachev, B. Barquera, Sequencing and preliminary characterization of the Na^+-translocating NADH:ubiquinone oxidoreductase from *Vibrio harveyi*, Biochemistry 38 (1999) 16246–16252.

[9] C.C. Häse, N.D. Fedorova, M.Y. Galperin, P.A. Dibrov, Sodium ion cycle in bacterial pathogens: evidence from cross-genome comparisons, Microbiol. Mol. Biol. Rev. 65 (2001) 353–370.
[10] Y. Nakayama, M. Hayashi, T. Unemoto, Identification of six subunits constituting Na^+-translocating NADH-quinone reductase from the marine *Vibrio alginolyticus*, FEBS Lett. 422 (1998) 240–242.
[11] P.R. Rich, B. Meunier, F.B. Ward, Predicted structure and possible ion-motive mechanism of the sodium-linked NADH-ubiquinone oxidoreductase of *Vibrio alginolyticus*, FEBS Lett. 375 (1995) 5–10.
[12] M. Hayashi, K. Hirai, T. Unemoto, Sequencing and the alignment of structural genes in the *nqr* operon encoding the Na^+-translocating NADH-quinone reductase from *Vibrio alginolyticus*, FEBS Lett. 363 (1995) 75–77.
[13] A.V. Bogachev, Y.V. Bertsova, B. Barquera, M.I. Verkhovsky, Sodium-dependent steps in the redox reactions of the Na^+-motive NADH:quinone oxidoreductase from *Vibrio harveyi*, Biochemistry 40 (2001) 7318–7323.
[14] B. Barquera, P. Hellwig, W. Zhou, J.E. Morgan, C.C. Häse, K.K. Gosink, M. Nilges, P.J. Bruesehoff, A. Roth, C.R. Lancaster, R.B. Gennis, Purification and characterization of the recombinant Na^+-translocating NADH:quinone oxidoreductase from *Vibrio cholerae*, Biochemistry 41 (2002) 3781–3789.
[15] M. Hayashi, T. Unemoto, FAD and FMN flavoproteins participate in the sodium-transport respiratory chain NADH:quinone reductase of a marine bacterium, *Vibrio alginolyticus*, FEBS Lett. 202 (1986) 327–329.
[16] X.D. Pfenninger-Li, S.P.J. Albracht, R. van Belzen, P. Dimroth, NADH:ubiquinone oxidoreductase of *Vibrio alginolyticus*: purification, properties, and reconstitution of the Na^+ pump, Biochemistry 35 (1996) 6233–6242.
[17] B. Barquera, W. Zhou, J.E. Morgan, R.B. Gennis, Riboflavin is a component of the Na^+-pumping NADH-quinone oxidoreductase from *Vibrio cholerae*, Proc. Natl. Acad. Sci. U. S. A. 99 (2002) 10322–10324.
[18] K. Turk, A. Puhar, F. Neese, E. Bill, G. Fritz, J. Steuber, NADH oxidation by the Na^+-translocating NADH:quinone oxidoreductase from *Vibrio cholerae*: functional role of the NqrF subunit, J. Biol. Chem. 279 (2004) 21349–21355.
[19] M.S. Casutt, T. Huber, R. Brunisholz, M. Tao, G. Fritz, J. Steuber, Localization and function of the membrane-bound riboflavin in the Na^+-translocating NADH:quinone oxidoreductase (Na^+-NQR) from *Vibrio cholerae*, J. Biol. Chem. 285 (2010) 27088–27099.
[20] R. Nedielkov, W. Steffen, J. Steuber, H.M. Moller, NMR reveals double occupancy of quinone-type ligands in the catalytic quinone binding site of the Na^+-translocating NADH:quinone oxidoreductase from *Vibrio cholerae*, J. Biol. Chem. 288 (2013) 30597–30606.
[21] A.V. Bogachev, Y.V. Bertsova, E.K. Ruuge, M. Wikström, M.I. Verkhovsky, Kinetics of the spectral changes during reduction of the Na^+-motive NADH:quinone oxidoreductase from *Vibrio harveyi*, Biochim. Biophys. Acta 1556 (2002) 113–120.
[22] O. Juárez, J.E. Morgan, B. Barquera, The electron transfer pathway of the Na^+-pumping NADH:quinone oxidoreductase from *Vibrio cholerae*, J. Biol. Chem. 284 (2009) 8963–8972.
[23] O. Juárez, B. Barquera, Insights into the mechanism of electron transfer and sodium translocation of the Na^+-pumping NADH:quinone oxidoreductase, Biochim. Biophys. Acta 1817 (2012) 1823–1832.
[24] M.I. Verkhovsky, A.V. Bogachev, A.V. Pivtsov, Y.V. Bertsova, M.V. Fedin, D.A. Bloch, L.V. Kulik, Sodium-dependent movement of covalently bound FMN residue(s) in Na^+-translocating NADH:quinone oxidoreductase, Biochemistry 51 (2012) 5414–5421.
[25] A.V. Bogachev, M.I. Verkhovsky, Na^+-translocating NADH:quinone oxidoreductase: progress achieved and prospects of investigations, Biochem. Mosc. 70 (2005) 143–149.
[26] E.B. Duffy, B. Barquera, Membrane topology mapping of the Na^+-pumping NADH:quinone oxidoreductase from *Vibrio cholerae* by PhoA-green fluorescent protein fusion analysis, J. Bacteriol. 188 (2006) 8343–8351.
[27] Y.V. Bertsova, A.V. Bogachev, The origin of the sodium-dependent NADH oxidation by the respiratory chain of *Klebsiella pneumoniae*, FEBS Lett. 563 (2004) 207–212.
[28] J.A. Peek, R.K. Taylor, Characterization of a periplasmic thiol:disulfide interchange protein required for the functional maturation of secreted virulence factors of *Vibrio cholerae*, Proc. Natl. Acad. Sci. U. S. A. 89 (1992) 6210–6214.
[29] P.K. Smith, R.I. Krohn, G.T. Hermanson, A.K. Mallia, F.H. Gartner, M.D. Provenzano, E.K. Fujimoto, N.M. Goeke, B.J. Olson, D.C. Klenk, Measurement of protein using bicinchoninic acid, Anal. Biochem. 150 (1985) 76–85.
[30] T. Watanabe, K. Honda, Measurement of the extinction coefficient of the methyl viologen cation radical and the efficiency of its formation by semiconductor photocatalysis, J. Phys. Chem. 86 (1982) 2617–2619.
[31] A.H. Ells, A colorimetric method for the assay of soluble succinic dehydogenase and pyridinenucleotide-linked dehydrogenases, Arch. Biochem. Biophys. 85 (1959) 561–562.
[32] M.S. Fadeeva, C. Nunez, Y.V. Bertsova, G. Espin, A.V. Bogachev, Catalytic properties of Na^+-translocating NADH:quinone oxidoreductases from *Vibrio harveyi*, *Klebsiella pneumoniae*, and *Azotobacter vinelandii*, FEMS Microbiol. Lett. 279 (2008) 116–123.
[33] G.W. Rafter, S.P. Colowick, Enzymatic preparation of DPNH and TPNH, Methods Enzymol. 3 (1957) 887–899.
[34] N.S. Naina, L.R. Gowda, S.G. Bhat, Preparation of NADH/NADPH using cetyltrimethylammonium bromide permeabilized baker's yeast cells, Anal. Biochem. 196 (1991) 234–237.
[35] M.S. Casutt, A. Schlosser, W. Buckel, J. Steuber, The single NqrB and NqrC subunits in the Na^+-translocating NADH:quinone oxidoreductase (Na^+-NQR) from *Vibrio cholerae* each carry one covalently attached FMN, Biochim. Biophys. Acta 1817 (2012) 1817–1822.
[36] U.K. Laemmli, Cleavage of structural proteins during the assembly of the head of bacteriophage T4, Nature 227 (1970) 680–685.
[37] D.E. Fouts, H.L. Tyler, R.T. DeBoy, S. Daugherty, Q. Ren, J.H. Badger, A.S. Durkin, H. Huot, S. Shrivastava, S. Kothari, R.J. Dodson, Y. Mohamoud, H. Khouri, L.F. Roesch, K.A. Krogfelt, C. Struve, E.W. Triplett, B.A. Methé, Complete genome sequence of the N_2-fixing broad host range endophyte *Klebsiella pneumoniae* 342 and virulence predictions verified in mice, PLoS Genet. 4 (2008) e1000141.
[38] J.M. Boyd, J.A. Endrizzi, T.L. Hamilton, M.R. Christopherson, D.W. Mulder, D.M. Downs, J.W. Peters, FAD binding by ApbE protein from *Salmonella enterica*: a new class of FAD-binding proteins, J. Bacteriol. 193 (2011) 887–895.
[39] A.S. Juncker, H. Willenbrock, G. von Heijne, H. Nielsen, S. Brunak, A. Krogh, Prediction of lipoprotein signal peptides in Gram-negative bacteria, Protein Sci. 12 (2003) 1652–1662.
[40] M. Punta, P.C. Coggill, R.Y. Eberhardt, J. Mistry, J. Tate, C. Boursnell, N. Pang, K. Forslund, G. Ceric, J. Clements, A. Heger, L. Holm, E.L. Sonnhammer, S.R. Eddy, A. Bateman, R.D. Finn, The Pfam protein families database, Nucleic Acids Res. 40 (2012) D290–D301.
[41] P.S. Dobbin, J.N. Butt, A.K. Powell, G.A. Reid, D.J. Richardson, Characterization of a flavocytochrome that is induced during the anaerobic respiration of Fe^{3+} by *Shewanella frigidimarina* NCIMB400, Biochem. J. 342 (1999) 439–448.
[42] C.J. Morris, A.C. Black, S.L. Pealing, F.D.C. Manson, S.K. Chapman, G.A. Reid, D.M. Gibson, F.B. Ward, Purification and properties of a novel cytochrome: flavocytochrome *c* from *Shewanella putrefaciens*, Biochem. J. 302 (1994) 587–593.
[43] W. Buckel, R.K. Thauer, Energy conservation via electron bifurcating ferredoxin reduction and proton/Na^+ translocating ferredoxin oxidation, Biochim. Biophys. Acta 1827 (2013) 94–113.
[44] A.V. Bogachev, D.A. Bloch, Y.V. Bertsova, M.I. Verkhovsky, Redox properties of the prosthetic groups of Na^+-translocating NADH:quinone oxidoreductase. 2. Study of the enzyme by optical spectroscopy, Biochemistry 48 (2009) 6299–6304.
[45] C.C. Page, C.C. Moser, X. Chen, P.L. Dutton, Natural engineering principles of electron tunnelling in biological oxidation-reduction, Nature 402 (1999) 47–52.
[46] M.S. Fadeeva, Y.V. Bertsova, M.I. Verkhovsky, A.V. Bogachev, Site-directed mutagenesis of conserved cysteine residues in NqrD and NqrE subunits of Na^+-translocating NADH:quinone oxidoreductase, Biochem. Mosc. 73 (2008) 123–129.
[47] Y. Zhang, D.E. Fomenko, V.N. Gladyshev, The microbial selenoproteome of the Sargasso Sea, Genome Biol. 6 (2005) R37.
[48] Y. Zhang, V.N. Gladyshev, Trends in selenium utilization in marine microbial world revealed through the analysis of the global ocean sampling (GOS) project, PLoS Genet. 4 (2008) e1000095.
[49] A.V. Bogachev, R.A. Murtasina, V.P. Skulachev, The Na^+/e^- stoichiometry of the Na^+-motive NADH:quinone oxidoreductase in *Vibrio alginolyticus*, FEBS Lett. 409 (1997) 475–477.
[50] O. Juárez, J.E. Morgan, M.J. Nilges, B. Barquera, Energy transducing redox steps of the Na^+-pumping NADH:quinone oxidoreductase from *Vibrio cholerae*, Proc. Natl. Acad. Sci. U. S. A. 107 (2010) 12505–12510.
[51] D.P. Heuts, N.S. Scrutton, W.S. McIntire, M.W. Fraaije, What's in a covalent bond? On the role and formation of covalently bound flavin cofactors, FEBS J. 276 (2009) 3405–3427.
[52] P.M. Wood, Why do *c*-type cytochromes exist? FEBS Lett. 164 (1983) 223–226.
[53] S. Miller, J. Mekalanos, A novel suicide vector and its use in construction of insertion mutations: osmoregulation of outer membrane proteins and virulence determinants in *Vibrio cholerae* requires *tox*R, J. Bacteriol. 170 (1988) 2575–2583.
[54] M.F. Alexeyev, The pKNOCK series of broad-host-range mobilizable suicide vectors for gene knockout and targeted DNA insertion into the chromosome of gram-negative bacteria, Biotechniques 26 (1999) 824–828.